Dalton Transactions

PAPER

View Article Online
View Journal | View Issue

Cite this: *Dalton Trans.*, 2018, **47**, 15757

Reactivity of the diphosphinodithio ligated nickel(0) complex toward alkyl halides and resultant nickel(I) and nickel(II)–alkyl complexes†

Ailing Zhang, Congxiao Wang, Xiaoyu Lai, Xiaofang Zhai, Maofu Pang, Chen-Ho Tung and Wenguang Wang *

Received 4th August 2018,
Accepted 15th October 2018

DOI: 10.1039/c8dt03188f

rsc.li/dalton

Diphosphinodithio ligated complexes of nickel(0), nickel(I) and nickel(II)–alkyl with a reactivity relevant to the C–C bond formation were described. Stoichiometric reactions of the nickel(0) complex, [(P_2S_2)Ni] ([**1**]^0, P_2S_2 = ($Ph_2PC_6H_4CH_2S)_2(C_2H_4$)), with alkyl halides (RX) such as $C_6H_5CH_2Br$, $C_2H_3CH_2Br$, C_2H_5I and $(CH_3)_2CHI$ were investigated, from which the products were found to be highly dependent on the nature of RX used. Oxidative addition of $C_2H_3CH_2Br$ to [**1**]^0 provides the stable Ni(II)–alkyl complexes [**1**-allyl]$^+$. The reaction of [**1**]^0 with $C_6H_5CH_2Br$ proceeds through a radical pathway resulting in the formation of the nickel(I) complex [**1**]$^+$ and an organic homo-coupled product 1,2-diphenylethane. Oxidative addition of C_2H_5I or $(CH_3)_2CHI$ to [**1**]^0 can be achieved but it competes with the halogen atom abstraction reaction as found for $C_6H_5CH_2Br$. [**1**]^0 was shown to be an active catalyst for the coupling reactions of primary halides and alkyl Grignard reagents.

Introduction

With their high abundance, relatively low cost and environmentally friendly properties, versatile Ni-based catalysts have been extensively studied over the last decade.[1] They have demonstrated high efficiency in a wide range of valuable, intriguing and challenging transformations.[1,2] In particular, nickel catalysis in cross-coupling reactions, such as aryl–aryl coupling,[3] aryl–alkyl coupling,[4] and alkyl–alkyl coupling reactions,[5] has attracted significant interest. Recent advances in characterization techniques and computational studies have provided insight into Ni-mediated alkyl–alkyl cross-coupling reactions, in which Ni–alkyl complexes are considered to be the key intermediates.[5–8]

Owing to their propensity to exist in various oxidation states, Ni(0), Ni(I), Ni(II) and even Ni(III) species can be invoked in the catalysis of cross-coupling reactions. The general nickel-based elementary reactions involved in Ni catalysis are shown in Chart 1. A typical Ni(0)/Ni(II)-based catalytic cycle includes the elementary steps of oxidative addition of RX to Ni(0) species affording Ni(II)–alkyl complexes, followed by transmetallation and reductive elimination to provide the product (Chart 1, (a) and (b)).[9] The Ni(II)–alkyl complex can undergo Ni–C homolytic cleavage to form Ni(I) species and alkyl radicals (c), and this competes with the transmetallation process. In particular, Ni-mediated alkyl–aryl couplings can proceed through a radical chain pathway that involves a Ni(I)/Ni(II)/Ni(III) cycle.[10] It has been proposed that the Ni(I) complex reacts with alkyl electrophiles to release an alkyl radical (d),[5b,c] which then adds to the Ni(II)–aryl species generated by oxidative addition of aryl halides to Ni(0) or by the transmetallation from aryl

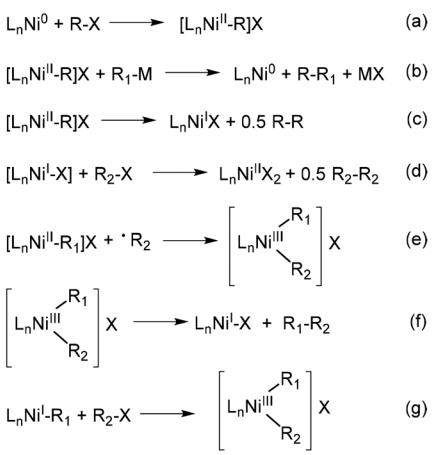

Chart 1 General Ni-centered elementary reactions involved in catalytic alkyl–alkyl and alkyl–aryl couplings.

Key Lab for Colloid and Interface Chemistry of Education Ministry, School of Chemistry and Chemical Engineering, Shandong University, Jinan 250100, PR China. E-mail: wwg@sdu.edu.cn

†Electronic supplementary information (ESI) available: Experimental procedures, characterization data and NMR spectra. CCDC 1840915–1840917. For ESI and crystallographic data in CIF or other electronic format see DOI: 10.1039/c8dt03188f

Grignard reagents to Ni(II) halides (e).[5b,c] The resulting Ni(III) species undergoes reductive elimination to give the coupling product, regenerating the Ni(I) complex (f).[7b,11] In the cases of aryl–aryl couplings catalyzed by nickel complexes bearing bulky NHC ligands,[12–14] it was proposed that aryl halides react with $Ni^0(NHC)_n$ species to generate the $(NHC)_nNi^I$–X compound. Transmetallation from the Grignard reagent R_1MgX' to $(NHC)_nNi(I)X$ provides $(NHC)_nNi(I)$-R_1 intermediates, followed by oxidative addition of aryl halide R_2X forming Ni(III) species (g). Apparently, there are multiple reaction pathways in Ni-catalyzed reactions due to the redox active nature of the nickel complexes,[1b,10] and the mechanism is dependent on the ligand employed. Therefore, it is of obvious interest and importance to synthesize nickel complexes in various oxidation states and examine their reactivity as it is related to the fundamental steps of Ni-mediated C–C couplings.

In our previous studies, we found that the four-coordinate dicationic $[(P_2S_2)Ni]^{2+}$ (P_2S_2 = $(Ph_2PC_6H_4CH_2S)_2(C_2H_4)$) complex reacts with CH_3MgBr forming the $[(P_2S_2)Ni–CH_3]^+$ complex which is active towards CO insertion.[15] In the present paper, we report the reactivity of $[(P_2S_2)Ni^0]$ toward alkyl halides and the resultant nickel(I) and nickel(II)–alkyl complexes, which are relevant to the C–C bond formation.

Results and discussion

$[(P_2S_2)Ni^0]$

The precursor complex $[(P_2S_2)Ni^0]$ ($[\mathbf{1}]^0$) was synthesized according to a published method with modifications.[15] Direct treatment of a solution in THF of P_2S_2 with a THF solution of $Ni(COD)_2$ provided the desired product, which was isolated as a red powder. Alternatively, complex $[\mathbf{1}]^0$ was prepared by the reduction of the Ni(II) complex $[(P_2S_2)Ni]^{2+}$($[\mathbf{1}]^{2+}$) with two equivalents of Cp_2Co. The ^{31}P NMR spectrum of $[\mathbf{1}]^0$ exhibits a phosphorus resonance at δ 21.3, compared to δ −16.9 for the free ligand P_2S_2. In the ^1H NMR spectrum of P_2S_2, the four PhCH_2 protons were displayed as a singlet at 3.89 ppm, which after complexation with Ni splits into two doublets at 3.06 and 3.51 ppm in THF-d_8.

X-ray quality crystals of $[\mathbf{1}]^0$ were grown from a THF/hexane solution. In the solid structure of $[\mathbf{1}]^0$, the Ni(0) center is in a distorted tetrahedral geometry suggested by the angles of 93.57(2)° for ∠S2–Ni1–S1 and 130.73(3)° for ∠P2–Ni1–P1 (Fig. 1). The two Ni–S bonds have almost identical bond lengths of 2.1939(6) and 2.1933(6), which compare well with 2.205 Å in $[(Ph_2PC_6H_4SMe)_2Ni]^0$.[16] The Ni–P distances of 2.1315(6) and 2.1205(6) Å are shorter than the Ni–S distances. In our earlier report, the nickel center in $Ni^{II}(P_2S_2)$ ($[\mathbf{1}]^{2+}$) adopts a distorted tetrahedral geometry.[15] Surprisingly, the average Ni–S distance in complex $[\mathbf{1}]^0$ is only about 0.007 Å longer when compared to that in $[\mathbf{1}]^{2+}$. In contrast to Ni–S > Ni–P in $[\mathbf{1}]^0$, in $(P_2S_2)Ni^{II}$ the Ni–P distances are longer than the Ni–S distances. Such differences agree with the changes reported for sulfur/phosphorus supported Ni(II) and Ni(0) species,[16] which probably are due to the better match of the soft/soft interaction of Ni(0) and P *vs.* the borderline hard/borderline soft interactions of Ni(II) and S.[16,17]

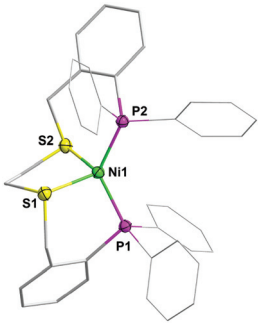

Fig. 1 Solid-state structure of $[\mathbf{1}]^0$. Thermal ellipsoids are shown at the 50% probability level, and hydrogen atoms are omitted for clarity. Selected distances (Å) and angles (°): Ni1–S1 = 2.1939(6), Ni1–S2 = 2.1933(6), Ni1–P1 = 2.1315(6), Ni1–P2 = 2.1205(6), S2–Ni1–S1 = 93.57(2), P1–Ni1–S1 = 101.15(2), P1–Ni1–S2 = 110.90(2), P2–Ni1–S1 = 113.26(2), P2–Ni1–S2 = 101.30(2), P2–Ni1–P1 = 130.73(3).

$[(P_2S_2)Ni^I]$

Addition of one equivalent of benzyl bromide (BnBr) to a solution of $[\mathbf{1}]^0$ in THF at room temperature resulted in a rapid color change from red to brown (eqn (1)). The organonickel complex was crystallized from a CH_2Cl_2/hexane solution overnight at −30 °C to afford yellow crystals, and the molecular structure was identified as $[(P_2S_2)Ni]BPh_4$ ($[\mathbf{1}]^+$) by X-ray crystallographic analysis.

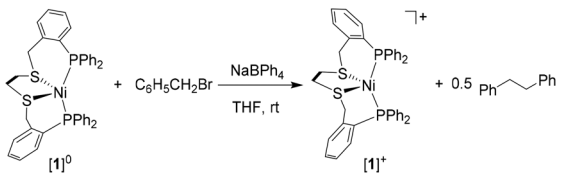

(1)

In the solid state, the framework of $[\mathbf{1}]^+$ is very similar to that of the nickel(0) precursor $[\mathbf{1}]^0$, and the Ni(I) center also adopts a tetrahedral geometry (Fig. 2). However, the structure of $[\mathbf{1}]^+$ is less compact than that of $[\mathbf{1}]^0$, and this is reflected by

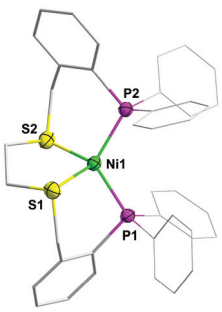

Fig. 2 Structure of $[\mathbf{1}]^+$. Selected distances (Å) and angles (°): Ni1–S1 = 2.2240(6), Ni1–S2 = 2.2160(7), Ni1–P1 = 2.2209(6), Ni1–P2 = 2.2095(6), S2–Ni1–S1 = 90.56(3), P1–Ni1–S1 = 96.48(2), P1–Ni1–S2 = 126.15(3), P2–Ni1–S1 = 126.90(3), P2–Ni1–S2 = 98.44(2), P2–Ni1–P1 = 117.97(2).

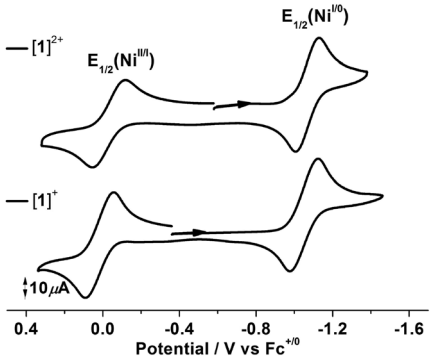

Fig. 3 Cyclic voltammogram for $[\mathbf{1}](BF_4)_2$ and $[\mathbf{1}]BPh_4$ in CH_2Cl_2. Conditions: 1 mM sample, 0.1 M Bu_4NPF_6; scan rate, 100 mV s^{-1}; potentials *vs.* $Fc^{+/0}$.

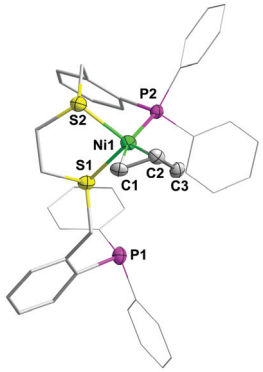

Fig. 4 Structure of [**1**-allyl]$^+$. Selected distances (Å) and angles (°): Ni1–S1 = 2.4446(7), Ni1–S2 = 2.2314(7), Ni1–P2 = 2.1913(7), Ni(1)–C(1) = 2.096(2), Ni(1)–C(2) = 1.997(3), Ni(1)–C(3) = 2.025(3), C(1)–C(2) = 1.393(4), C(2)–C(3) = 1.420(4), S2–Ni1–S1 = 87.90(2), P2–Ni1–S1 = 98.55(2), P2–Ni1–S2 = 97.02(3), C(1)–C(2)–C(3) = 117.4(3).

an increase in the average Ni–S distance and the Ni–P distance by 0.026 and 0.089 Å, respectively, together with the enlarged ∠P1–Ni1–S2 (126.15(3)°). The solution magnetic moment of $[\mathbf{1}]^+$ is 1.79μ_B at room temperature, which is consistent with the expected d^9 configuration.[18]

The cyclic voltammogram of $[\mathbf{1}]^+$ was recorded in CH_2Cl_2 to compare its redox properties with those of $[\mathbf{1}]^{2+}$ (Fig. 3). Complex $[\mathbf{1}]^+$ exhibits two reversible redox peaks at 0.02 V (i_{pc}/i_{pa} = 1.00) and −1.05 V (i_{pc}/i_{pa} = 1.02). Cyclic voltammetry of $[\mathbf{1}]^{2+}$ demonstrated two similar reversible electrochemical processes for $[\mathbf{1}]^+$. Accordingly, the first redox event at 0.02 V is assigned to the Ni^{II}/Ni^{I} couple and the second one at −1.05 V to the Ni^{I}/Ni^{0} couple. The stability of $[\mathbf{1}]^+$ and $[\mathbf{1}]^0$ is reflected by the readily reversible redox properties.

Reactions of Ni(0) species with aryl or alkyl halides can proceed in a multiplicity of pathways such as electron transfer and oxidative addition, affording a diversity of products.[19] For example, reactions of $Ni(PEt_3)_4$ and aryl halides produce a mixture of Ni(I) and the oxidative addition product ArNiX.[3c] According to the ESI-MS spectral analysis, the organonickel product for the stoichiometric reaction between $[\mathbf{1}]^0$ and $PhCH_2Br$ was $[\mathbf{1}]^+$; however, the formation of the oxidative addition product $[\mathbf{1}\text{-}CH_2Ph]^+$ was not evidenced. In addition to $[\mathbf{1}]^+$, the organic product is 1,2-diphenylethane, which was identified by ^{1}H NMR spectroscopy and GC-MS analysis (Fig. S5 and S6†). We proposed that the reaction of $[\mathbf{1}]^0$ and $PhCH_2Br$ proceeds through a radical pathway resulting in the formation of $[\mathbf{1}]^+$ and a benzyl radical.[20] We also found that $[\mathbf{1}]^+$ can further react with $PhCH_2Br$ to give $[\mathbf{1}]^{2+}$ and 1,2-diphenylethane, which were confirmed respectively by ^{31}P NMR spectroscopy and GC-MS analysis. A similar one-electron transfer type mechanism has been reported for the macrocyclic nickel(I) complex $[Ni(tmc)]^+$ with alkyl halides.[19]

[1-allyl]$^+$

Treatment of $[\mathbf{1}]^0$ with allyl bromide in THF followed by anion exchange with $NaBPh_4$ resulted in the formation of [**1**-allyl]BPh_4, identified by ^{1}H NMR, ^{31}P NMR spectroscopy and X-ray crystallography (Fig. 4). The ^{1}H NMR spectrum showed a characteristic peak at 6.02 ppm corresponding to the allyl proton (Fig. S8†).[24] Two phosphorus signals (20.2 ppm and −18.2 ppm) were displayed in the ^{31}P NMR spectrum, suggesting the decoordination of one of the P atoms from the Ni(II) center. Crystallographic analysis confirmed the anticipated structure of [**1**-allyl]$^+$ in which the allyl group is bound to nickel in a η^3 mode. The Ni–C distances are nearly equal (Ni1–C1 2.096(2) Å, Ni1–C2 1.997(3) Å and Ni1–C3 2.025(3) Å), and the C–C bond lengths in the allyl group differ by only 0.027 Å (d_{C1-C2} = 1.393(4) Å *vs.* d_{C2-C3} = 1.420(4) Å). The Ni(II) center exhibits an 18-electron configuration. In addition to the allyl group, the nickel center is also coordinated to the two S atoms and one P atom of the P_2S_2 ligand. It is worth noting that in our previously reported Ni(0)–CO system, one of the S atoms is not coordinated to the metal center.[15] These present results reveal the coordination flexibility of the P_2S_2 ligand in the stabilization of nickel complexes.

It is well known that metal–allyl complexes undergo dynamic conversions between η^3- and η^1-forms.[25,26] The dynamic behavior of the allyl group in [**1**-allyl]$^+$ was demonstrated by VT NMR experiments. As seen in Fig. 5, lowering the temperature of the CD_2Cl_2 solution of [**1**-allyl]$^+$ led to decalescence of the ^{1}H NMR spectrum, suggesting that a dynamic process is involved in the system. The central proton H_a in the allyl group appeared as a characteristic quintet at 6.02 ppm at room temperature, and the chemical shift is not temperature-dependent, which is consistent with the dynamic interconversion of a η^3–η^1 rearrangement reported for the Ni(II)–allyl systems.[26] At room temperature, the *syn* protons (H_b and H'_b) and *anti* protons (H_c and H'_c) together yielded broad signals.[24,25] When the temperature was decreased to 213 K, the *syn* and *anti* protons were resolved into four sharp doublets at δ 3.14, 2.86, 2.79 and 2.58. In the ^{31}P NMR spectra, two broad peaks were observed at room temperature, and they became sharper at lower temperatures. It is likely that one P atom remains uncoordinated in the η^1 complex and this is probably due to the steric hindrance from the phenyl groups and the alkyl group.

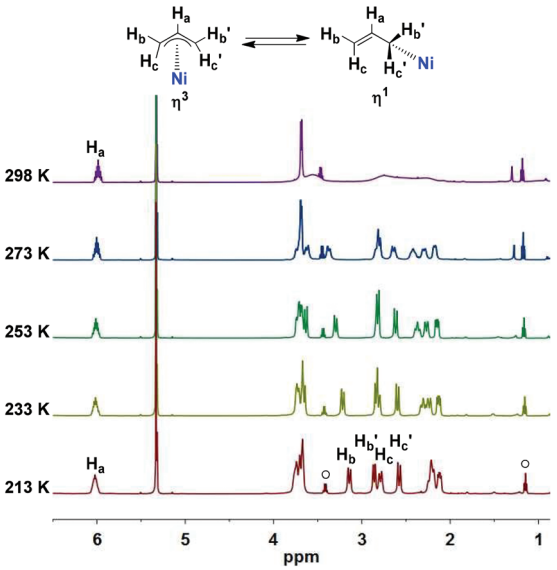

Fig. 5 VT ^{1}H NMR (500 MHz, CD_2Cl_2) of [**1**-allyl]BPh_4 (○ = diethyl ether).

Reactions of $[(P_2S_2)Ni^0]$ with C_2H_5I and $(CH_3)_2CHI$

The reactivity of $[\mathbf{1}]^0$ toward less activated alkyl halides such as iodoethane and 2-iodopropane was also examined. The reactions of $[\mathbf{1}]^0$ with C_2H_5I or $(CH_3)_2CHI$ were performed in THF followed by treatment with $NaBPh_4$. ESI-MS studies of the reaction solutions indicated the production of organonickel species $[\mathbf{1}\text{-Et}]^+$ and $[\mathbf{1}\text{-}^i\text{Pr}]^+$, respectively (Scheme 1a). For the reaction of $[\mathbf{1}]^0$ with CD_3CD_2I, the ESI-MS spectrum analysis featured an ionic peak at *m*/*z* 734.1768 for $[\mathbf{1}\text{-}C_2D_5]^+$ *vs.* *m*/*z* 729.1457 for $[\mathbf{1}\text{-Et}]^+$. The isotopic distribution agrees well with the calculated values. The product was precipitated by diluting the reaction solution with Et_2O. The ^{1}H NMR spectrum of $[\mathbf{1}\text{-Et}]^+$ displayed the Ni–CH_2CH_3 signals at δ 1.97 (q, 2H) and δ 1.03 (t, 3H), compared to the ^{2}H resonances at δ 1.95 and 0.99 observed for the deuteride $[\mathbf{1}\text{-}C_2D_5]^+$ in CH_2Cl_2. We found that $[\mathbf{1}\text{-Et}]^+$ underwent degeneration to provide $[\mathbf{1}\text{-H}]^+$ and ethylene (eqn (2), Fig. S16†). As monitored by the ^{1}H NMR spectrum, the production of ethylene was signaled at δ 5.40,[21] while the characteristic hydride signal of $[\mathbf{1}\text{-H}]^+$ was displayed at δ −13.8.[15]

$$\underset{[\mathbf{1}\text{-Et}]^+}{[(P_2S_2)\text{Ni-Et}]^+} \xrightarrow[\text{rt}]{CD_2Cl_2} \underset{[\mathbf{1}\text{-H}]^+}{[(P_2S_2)\text{Ni-H}]^+} + C_2H_4 \qquad (2)$$

ESI-MS spectral analysis for the reaction solution of $[\mathbf{1}]^0$ with $(CH_3)_2CHI$ showed a peak at *m*/*z* 743.1600 matching well with the calculated value for $[\mathbf{1}\text{-}^i\text{Pr}]^+$ (Fig. S26†). In the ^{1}H NMR spectrum of $[\mathbf{1}\text{-}^i\text{Pr}]^+$, the methine proton Ni–C*H*$(CH_3)_2$ exhibits a well-resolved septet at δ 2.39, while the methyl groups appear as a doublet at δ 0.96 (J_{H-H} = 5.2 Hz). Intensive efforts to obtain high-quality single crystals suitable for X-ray crystallographic analysis that would provide the solid-state structure of $[\mathbf{1}\text{-}^i\text{Pr}]^+$ or $[\mathbf{1}\text{-Et}]^+$, however, were unsuccessful. According to ^{31}P NMR spectra, the ^{31}P resonances of $[\mathbf{1}\text{-}^i\text{Pr}]^+$ and $[\mathbf{1}\text{-Et}]^+$ are similar to the patterns observed for $[\mathbf{1}\text{-Me}]^+$ at low temperature.[15] The ^{31}P NMR spectrum of $[\mathbf{1}\text{-}^i\text{Pr}]^+$ showed phosphorus resonances as two doublets at δ 44.06 and 12.76 with J_{P-P} = 207.8 Hz, which are comparable to the ^{31}P signals at δ 40.45 and 9.81 with J_{P-P} = 201.1 Hz for $[\mathbf{1}\text{-Et}]^+$. Although the phosphorus resonances of $[\mathbf{1}\text{-Me}]^+$ were displayed as a broad peak (δ 12.98) at room temperature,[15] it split into two peaks at δ 16.78 and δ 7.38 when the temperature was decreased to 253 K. At a lower temperature of 213 K, the ^{31}P signals were well resolved as two doublets with J_{P-P} = 177.5 Hz (Fig. S29†), consistent with the pseudo-trigonal–bipyramidal geometry reported for the solid-state structure of $[\mathbf{1}\text{-Me}]^+$. The two non-equivalent phosphorus atoms in $[\mathbf{1}\text{-Me}]^+$ are also reflected by the striking differences in the Ni–P distances (Δ(Ni–P) = 0.1 Å).[15]

In addition to the expected oxidative addition product $[\mathbf{1}\text{-R}]^+$, it is more likely that reactions of $[\mathbf{1}]^0$ with C_2H_5I and $(CH_3)_2CHI$ also involve halogen atom abstraction to form nickel(I) species and alkyl radicals (Scheme 1b).[22] The reaction mixture of $[\mathbf{1}]^0$ and the alkyl iodide was always NMR silent, indicating the production of paramagnetic species. Recrystallization of the reaction residue at −30 °C provided single crystals and some of these were confirmed to be $[\mathbf{1}]^+$ by crystallographic analysis. Although homolytic cleavage of the Ni–C bond of Ni(II)–alkyl complexes is known,[19,20,22] it should be noted that the decomposition of $[\mathbf{1}\text{-Et}]^+$ only provided Ni(II)–H hydride species and C_2H_4, at least according to ^{1}H NMR spectroscopic studies. Unlike $[\mathbf{1}\text{-Et}]^+$, the degeneration of $[\mathbf{1}\text{-}^i\text{Pr}]^+$ to $[\mathbf{1}\text{-H}]^+$ was not observed by ^{1}H NMR spectral studies (Fig. S27†).

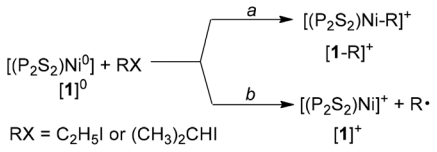

Scheme 1 Possible reaction pathways for $[\mathbf{1}]^0$ with iodoethane and 2-iodopropane.

Reactivity of Ni(II)–alkyl complexes towards Grignard reagents

The stoichiometric reaction of $[\mathbf{1}\text{-Et}]^+$ with PhMgBr was subsequently examined. $[\mathbf{1}\text{-Et}]^+$ was formed *in situ* by the reaction of CH_3CH_2I with $[\mathbf{1}]^0$ monitored by ^{31}P NMR spectroscopy, after which the Grignard reagent was added. The formation of the desired C–C coupled product $C_6H_5C_2H_5$ was analysed by ^{1}H NMR and GC-FID, while the regeneration of $[\mathbf{1}]^0$ was confirmed by ^{31}P NMR spectroscopy (Fig. S31†). The results indicate that $[\mathbf{1}\text{-Et}]^+$ is an active intermediate in the C–C bond formation through transmetallation. Based on the stoichiometric reaction, we found that $[\mathbf{1}]^0$ is capable of catalysing the coupling reaction between CH_3CH_2I and PhMgBr. With 2 mol% of $[\mathbf{1}]^0$, the reaction of CH_3CH_2I and PhMgBr in d_8-THF completed in 15 min, as suggested by the disappearance of proton signals of CH_3CH_2I in the ^{1}H NMR spectrum (Fig. S36†). In addition to $C_6H_5C_2H_5$ (60% yield), the reaction indeed produces butane with the characteristic peaks at δ 1.27 (m) and

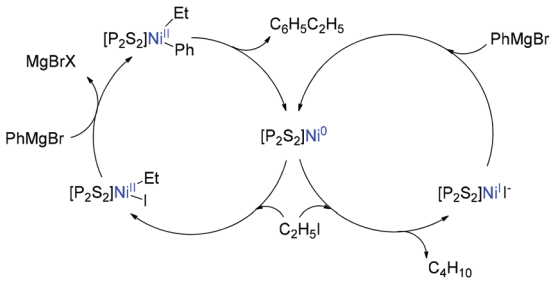

Scheme 2 The proposed catalytic cycle for alkyl–aryl coupling by $[\mathbf{1}]^0$.

δ 0.87 (t, J_{H-H} = 6.9 Hz).[22,28] By contrast, the conversion of CH_3CH_2I for the reaction of CH_3CH_2I and PhMgBr without $[\mathbf{1}]^0$ is only 16%, and the production of butane was not detected. These results confirm that halogen atom abstraction by $[\mathbf{1}]^0$ competes with oxidative addition of CH_3CH_2I to $[\mathbf{1}]^0$ (Scheme 2).

(3)

It is well known that alkyl–aryl coupling is more favoured than alkyl–alkyl coupling in classic Pd and Ni-catalyzed cross-coupling reactions.[1a] Notably, $[\mathbf{1}]^0$ can also promote the activation of C_{sp^3}–X bonds and can catalyse the cross-coupling reactions of primary alkyl halides with alkyl Grignard reagents (eqn (3)). TMEDA (tetramethylethylenediamine) was added to the reaction mixture to increase the stability of the functionalized Grignard reagent.[23] With only 2 mol% of $[\mathbf{1}]^0$, the reaction of (2-iodoethyl)-benzene and *n*-BuMgCl proceeded successfully in 2 h at 0 °C, giving the desired C–C coupled product in 74% yield (eqn (3)). Switching the substrate to an alkyl ether iodide $C_6H_5OC_3H_6I$, the catalysis also provided the desired product in a reasonable yield (67%). Utilization of a primary alkyl bromide $C_6H_5OC_3H_6Br$ resulted in a significantly decreased yield of 42% because of the difficulty of C–Br bond activation compared to a C–I bond (entry 3, Table S1†). Although $[\mathbf{1}]^0$ is an active catalyst for the alkyl–aryl coupling reactions, the competing radical pathway of halogen atom abstraction leading to the formation of a alkyl–alkyl by-product is considered to be a major impediment to efficient alkyl electrophile cross-coupling (Scheme 2).

Conclusions

Reactions of the nickel(0) compound with alkyl halides were examined, and the products were found to depend on the nature of RX used. $[(P_2S_2)Ni^0]$ is an active catalyst for coupling reactions with primary halides and Grignard reagents, for which the Ni^{II}–alkyl species formed by oxidative addition of alkyl halides are envisioned to be the key intermediates. The soft and flexible coordination properties of the diphosphinodithio tetradentate ligand are reflected by its character in the stabilization of nickel complexes with oxidation states of 0, I and II. It should be noted that transition metal–methyl bonds tend to be stronger than those of higher alkyl ligands, and the metal–alkyl bond strength is significantly affected by steric factors.[27]

Experimental section

All manipulations were conducted under a N_2 atmosphere using standard Schlenk techniques or in a glovebox, unless otherwise stated. All reagents were purchased from Sigma-Aldrich, and used as received. $(P_2S_2)Ni$ ($[\mathbf{1}]^0$) was prepared according to our previous methods. Et_2O, pentane, THF (dried by distillation over sodium), MeCN (dried by distillation over CaH_2) and CH_2Cl_2 for general use were of AR grade and stored under an atmosphere of N_2. CD_2Cl_2 was dried using activated molecular sieves (4 Å) and degassed with three thaw–freeze cycles. C_6D_6 was dried over CaH_2 and distilled by vacuum transfer. NMR spectra were recorded on a Bruker Avance 500 spectrometer in J. Young NMR tubes. ^1H, ^{13}C and ^{31}P NMR chemical shifts are referenced to the residual solvent peak of the deuterated solvent and external H_3PO_4, respectively. Cyclic voltammetry was performed under N_2 at room temperature using a CHI 760e electrochemical workstation (Shanghai Chen Hua Instrument Co., Ltd) with a glassy carbon working electrode, Pt wire counter electrode, and the pseudo-reference electrode Ag wire. HRMS were recorded on a commercial instrument (ESI Source).

Synthesis of $(P_2S_2)Ni$, $[\mathbf{1}]^0$

Method a. $[\mathbf{1}]^0$ was prepared according to our published methods.[15] A solution of $Ni(COD)_2$ (0.141 g, 0.51 mmol) in THF (10 mL) was added dropwise to a solution of $(Ph_2PC_6H_4CH_2S)_2(C_2H_4)$ (0.300 g, 0.47 mmol) in THF (20 mL) over the course of 5 min. The mixture was stirred for 10 min, and then the solvent was removed under vacuum. The residue was washed with Et_2O (3 × 5 mL), and then dried under vacuum to give the product as a dark red solid (0.278 g, 85% yield). Single crystals suitable for X-ray diffraction were obtained by layering hexane into a saturated THF solution of the product at −30 °C. ^1H NMR (500 MHz, THF-d_8): δ 7.63–6.79 (m, 28 × Ar*H*), 3.51 (br, 2H, SCH_2Ph), 3.06 (br, 2H, SCH_2Ph), 2.53 (br, 2H, SCH_2CH_2S), 1.40 (s, 2H, SCH_2CH_2S). $^{31}P\{^1H\}$ NMR (202 MHz, toluene, H_3PO_4 as internal standard): δ 21.28 (s). Anal. Calcd for $C_{40}H_{36}NiP_2S_2$: C, 68.49; H, 5.17. Found: C, 68.55; H, 5.29. ESI-MS: calcd for $[\mathbf{1}]^0$: 700.1087; found: 700.1071.

Method b. $[(P_2S_2)Ni]^{2+}$ was prepared according to literature procedures.[15] Cp_2Co (0.086 g, 0.46 mmol) in THF (10 mL) was added to a solution of complex $[(P_2S_2)Ni]^{2+}$ (0.200 g, 0.23 mmol) in THF (15 mL). The mixture was stirred at room temperature until the Ni(II) compound was reduced, and the color of the solution changed from red to deep red. The

mixture was immediately filtered through a short pad of Celite, and the filtrate was dried under vacuum. The product was extracted by toluene (3 × 5 mL) and dried under vacuum to afford (P_2S_2)Ni as a dark red solid. (0.130 g, 81% yield).

Reaction of $[(P_2S_2)Ni^0]$ with benzyl bromide

Benzyl bromide (18.6 μL, 0.16 mmol) was added into a solution of $[\mathbf{1}]^0$ (0.100 g, 0.14 mmol) in THF, resulting in a rapid color change from red to brown. Then, a solution of $NaBPh_4$ (0.059 g, 0.17 mmol) in THF (5 mL) was added to the reaction mixture. After being vigorously stirred for 10 min, the reaction mixture was filtered through Celite, and the filtrate was subjected to mass spectroscopy (ESI-MS and GC-MS) and NMR spectroscopy analyses. Finally, the filtrate was dried under vacuum, and the residue was recrystallized from CH_2Cl_2/hexane overnight at −30 °C, providing $[(P_2S_2)Ni]BPh_4$ ($[\mathbf{1}]^+$) as yellow crystals (0.131 g, 90% yield). μ_{eff} (Evans): 1.79μ_B. Anal. Calcd for $C_{64}H_{56}BNiP_2S_2$: C, 75.31; H, 5.53. Found: C, 75.45; H, 5.62. ESI-MS: calcd for $[\mathbf{1}]^+$: 700.1087; found: 700.1068.

Reaction of $[(P_2S_2)Ni^0]$ with allyl bromide

Allyl bromide (13.6 μL, 0.16 mmol) was added into a solution of $[\mathbf{1}]^0$ (0.100 g, 0.14 mmol) in THF at room temperature. Then, a solution of $NaBPh_4$ (0.059 g, 0.17 mmol) in THF (5 mL) was added to the reaction mixture. After being vigorously stirred for 10 min, the reaction mixture was filtered through Celite. The filtrate was subjected to mass spectroscopy (ESI-MS) and NMR spectroscopy analyses. The filtrate was subsequently dried under vacuum, and the residue was extracted with CH_2Cl_2. The resulting CH_2Cl_2 solution was concentrated, layered with hexane and cooled at −30 °C to give dark red crystals. Yield: 124 mg (82%). ^{1}H NMR (500 MHz, CD_2Cl_2, 213 K): δ 8.38–6.57 (m, 48 × Ar*H*), 6.02 (m, 1H, allyl H_a), 3.70 (m, 4H, SCH_2Ph), 3.14 (d, 1H, allyl H_b), 2.86 (d, 1H, allyl H'_b), 2.79 (d, 1H, allyl H_c), 2.58 (d, 1H, allyl H'_c), 2.21 (t, 2H, SCH_2CH_2S), 2.12 (dd, 1H, SCH_2CH_2S), 0.47 (m, 1H, SCH_2CH_2S). $^{31}P\{^1H\}$ NMR (202 MHz, CD_2Cl_2, 213 K): δ 20.24 (s), −20.58 (s). $^{31}P\{^1H\}$ NMR (202 MHz, CD_2Cl_2, 298 K): δ 20.21 (s), −18.20 (s). $^{13}C\{^1H\}$ NMR (126 MHz, CD_2Cl_2): δ 103.74 (s, allyl C2), 62.96 (br s, allyl C1), 37.68 (br s, allyl C3). Anal. Calcd for $C_{67}H_{61}BNiP_2S_2$: C, 75.79; H, 5.79. Found: C, 75.88; H, 5.87. ESI-MS: calcd for [**1**-allyl]$^+$: 741.1478; found: 741.1458.

Reaction of $[(P_2S_2)Ni^0]$ with C_2H_5I or C_2D_5I

$[\mathbf{1}]^0$ (0.100 g, 0.14 mmol) and iodoethane (12.6 μL, 0.16 mmol) were dissolved in THF (15 mL). The mixture was then was treated with $NaBPh_4$ (0.059 g, 0.17 mmol) and stirred at room temperature for 15 min. The reaction mixture was filtered through Celite, and the filtrate was subjected to mass spectroscopy (ESI-MS) and NMR spectroscopy analyses. The filtrate was subsequently dried under vacuum, and the residue was extracted with CH_2Cl_2. The product was obtained as a red solid by evaporating the solvent. (0.101 g, 68% yield). ESI-MS: calcd for [**1**-Et]$^+$: 729.1478; found, 729.1457. ^{1}H NMR (500 MHz, CD_2Cl_2): δ 7.31–6.86 (m, 48 × Ar*H*), 3.23 (br, 4H, SCH_2Ph), 2.86 (br, 2H, SCH_2CH_2S), 2.21 (br, 2H, SCH_2CH_2S), 1.97 (q, J = 7.1 Hz, 2H, CH_2CH_3), 1.03 (t, J = 7.1 Hz, 3H, CH_2CH_3). $^{31}P\{^1H\}$ NMR (202 MHz, CD_2Cl_2): δ 40.45 (d, J_{PP} = 201.1 Hz), 9.81 (d, J_{PP} = 201.1 Hz). Anal. Calcd for $NiP_2S_2C_{66}H_{61}B$: C, 75.51; H, 5.86. Found: C, 75.63; H, 5.95.

ESI-MS: calcd for [**1**-C_2D_5]$^+$: 734.1792; found, 734.1768. ^{2}H NMR (CH_2Cl_2): δ 1.95 (br, Ni–CD_2CD_3), 0.99 (br, Ni–CD_2CD_3). $^{31}P\{^1H\}$ NMR (202 MHz, CH_2Cl_2): δ 40.52 (d, J_{P-P} = 198.2 Hz), 9.53 (d, J_{P-P} = 198.2 Hz).

Reaction of $[(P_2S_2)Ni^0]$ with $(CH_3)_2CHI$

The reaction of $[(P_2S_2)Ni^0]$ with 2-iodopropane was followed by a similar procedure utilized for C_2H_5I with $[(P_2S_2)Ni^0]$. Yield: 0.093 g (61%). ESI-MS: calcd for [**1**-^{i}Pr]$^+$: 743.1635; found, 743.1600. ^{1}H NMR (500 MHz, CD_2Cl_2): δ 7.60–6.86 (m, 48 × Ar*H*), 3.32 (br, 2H, SCH_2Ph), 2.88 (d, 2H, SCH_2Ph), 2.39 (sept, 1H, CH(CH$_3$)$_2$), 2.15 (br, 2H, SCH_2CH_2S), 1.66 (br, 2H, SCH_2CH_2S), 0.96 (d, 6H, CH(CH_3)$_2$) $^{31}P\{^1H\}$ NMR (202 MHz, CD_2Cl_2): δ 44.06 (d, J_{P-P} = 207.8 Hz), 12.76 (d, J_{P-P} = 207.8 Hz). $^{31}P\{^1H\}$ NMR (202 MHz, CD_2Cl_2, 213 K): δ 48.14 (d, J = 196.8 Hz), 13.48 (d, J = 196.8 Hz). $^{13}C\{^1H\}$ NMR (126 MHz, CD_2Cl_2): δ 164.20, 136.34, 133.94, 133.85, 133.70, 132.39, 132.30, 132.18, 132.12, 131.79, 131.73, 131.58, 131.46, 131.01, 129.92, 129.34, 129.14, 128.05, 128.00, 127.89, 127.69, 126.68, 125.91, 122.05, 37.72, 37.59, 35.30, 35.16, 29.91, 27.04, 22.38. Anal. Calcd for $C_{67}H_{63}BNiP_2S_2$: C, 75.65; H, 5.97. Found: C, 75.63; H, 6.10.

General procedures for catalytic cross-coupling reactions

A mixture of alkyl halide (0.5 mmol), (P_2S_2)Ni (0.007 g, 0.01 mmol), and TMEDA (22.6 μL, 0.15 mmol) was dissolved in THF (1 mL) in a glovebox. 1,3,5-Trimethoxybenzene (10 mg) was added to this solution as an internal standard. RMgX (0.5 mmol) was added dropwise to the reaction mixture at 0 °C. The reaction mixture was stirred for 2 h, after which the NMR sample was prepared using 0.05 mL of the reaction mixture in 0.5 mL of $CDCl_3$.

Conflicts of interest

There are no conflicts to declare.

Acknowledgements

This work is supported by the "Thousand Plan" Youth Program and the National Natural Science Foundation of China (21871166 and 91427303).

Notes and references

1 (*a*) A. M. Echavarren and D. J. Cardenas, in *Metal-Catalyzed Cross-Coupling Reactions*, ed. A. de Meijere and F. Diederich, Wiley, VCH, 2nd edn, 2004, ch. 1, pp. 1–40;

(*b*) S. Z. Tasker, E. A. Standley and T. F. Jamison, *Nature*, 2014, **509**, 299–309; (*c*) S. Chakraborty, P. Bhattacharya, H. G. Dai and H. R. Guan, *Acc. Chem. Res.*, 2015, **48**, 1995–2003.

2 (*a*) C.-Y. Lin and P. P. Power, *Chem. Soc. Rev.*, 2017, **46**, 5347–5399; (*b*) J. R. Zhou and G. C. Fu, *J. Am. Chem. Soc.*, 2004, **126**, 1340–1341; (*c*) Z. Lu and G. C. Fu, *Angew. Chem., Int. Ed.*, 2010, **49**, 6676–6678; (*d*) X. L. Hu, *Chem. Sci.*, 2011, **2**, 1867–1886; (*e*) X. F. Jia, M. R. Zhang, M. H. Li, F. Pan, K. L. Ding, L. Jia, L. A. Crandall, J. T. Engle and C. J. Ziegler, *Organometallics*, 2017, **36**, 1122–1132; (*f*) E. M. Matson, G. Espinosa Martinez, A. D. Ibrahim, B. J. Jackson, J. A. Bertke and A. R. Fout, *Organometallics*, 2015, **34**, 399–407.

3 (*a*) J. Yamaguchi, K. Muto and K. Itami, *Eur. J. Org. Chem.*, 2013, 19–30; (*b*) M. Tobisu, T. Xu, T. Shimasaki and N. Chatani, *J. Am. Chem. Soc.*, 2011, **133**, 19505–19511; (*c*) T. T. Tsou and J. K. Kochi, *J. Am. Chem. Soc.*, 1979, **101**, 6319–6332; (*d*) Y. Q. Sun, X. Y. Li and H. J. Sun, *Dalton Trans.*, 2014, **43**, 9410–9413; (*e*) M. C. Schwarzer, R. Konno, T. Hojo, A. Ohtsuki, K. Nakamura, A. Yasutome, H. Takahashi, T. Shimasaki, M. Tobisu, N. Chatani and S. Mori, *J. Am. Chem. Soc.*, 2017, **139**, 10347–10358; (*f*) M. M. Beromi, A. Nova, D. Balcells, A. M. Brasacchio, G. W. Brudvig, L. M. Guard, N. Hazari and D. J. Vinyard, *J. Am. Chem. Soc.*, 2017, **139**, 922–936.

4 (*a*) D. J. Weix, *Acc. Chem. Res.*, 2015, **48**, 1767–1775; (*b*) C. Lévêque, L. Chenneberg, V. Corcé, J.-P. Goddard, C. Ollivier and L. Fensterbank, *Org. Chem. Front.*, 2016, **3**, 462–465; (*c*) M. O. Konev, L. E. Hanna and E. R. Jarvo, *Angew. Chem., Int. Ed.*, 2016, **55**, 6730–6733; (*d*) L. Peng, Z. Q. Li and G. Y. Yin, *Org. Lett.*, 2018, **20**, 1880–1883; (*e*) K. E. Poremba, N. T. Kadunce, N. Suzuki, A. H. Cherney and S. E. Reisman, *J. Am. Chem. Soc.*, 2017, **139**, 5684–5687; (*f*) T. Iwasaki, A. Fukuoka, W. Yokoyama, X. Min, I. Hisaki, T. Yang, M. Ehara, H. Kuniyasu and N. Kambe, *Chem. Sci.*, 2018, **9**, 2195–2211.

5 (*a*) J. R. Zhou and G. C. Fu, *J. Am. Chem. Soc.*, 2003, **125**, 14726–14727; (*b*) A. S. Dudnik and G. C. Fu, *J. Am. Chem. Soc.*, 2012, **134**, 10693–10697; (*c*) S. L. Zultanski and G. C. Fu, *J. Am. Chem. Soc.*, 2013, **135**, 624–627; (*d*) O. Vechorkin and X. L. Hu, *Angew. Chem., Int. Ed.*, 2009, **48**, 2937–2940; (*e*) Z. Csok, O. Vechorkin, S. B. Harkins, R. Scopelliti and X. L. Hu, *J. Am. Chem. Soc.*, 2008, **130**, 8156–8157; (*f*) J. Choi and G. C. Fu, *Science*, 2017, **356**, eaaf7230; (*g*) X. Mu, Y. Shibata, Y. Makida and G. C. Fu, *Angew. Chem., Int. Ed.*, 2017, **56**, 5821–5824.

6 Z. Li and L. Liu, *Chin. J. Catal.*, 2015, **36**, 3–14.

7 (*a*) O. Vechorkin, Z. Csok, R. Scopelliti and X. L. Hu, *Chem. – Eur. J.*, 2009, **15**, 3889–3899; (*b*) M. I. Lipschutz and T. D. Tilley, *Angew. Chem., Int. Ed.*, 2014, **53**, 7290–7294; (*c*) T. J. Anderson, G. D. Jones and D. A. Vicic, *J. Am. Chem. Soc.*, 2004, **126**, 8100–8101; (*d*) B. Zheng, F. Z. Tang, J. Luo, J. W. Schultz, N. P. Rath and L. M. Mirica, *J. Am. Chem. Soc.*, 2014, **136**, 6499–6504.

8 (*a*) G. T. Venkanna, S. Tammineni, H. D. Arman and Z. J. Tonzetich, *Organometallics*, 2013, **32**, 4656–4663; (*b*) L.-C. Liang, W.-Y. Lee, Y.-T. Hung, Y.-C. Hsiao, L.-C. Cheng and W.-C. Chen, *Dalton Trans.*, 2012, **41**, 1381–1388; (*c*) L.-C. Liang, P.-S. Chien, J.-M. Lin, M.-H. Huang, Y.-L. Huang and J.-H. Liao, *Organometallics*, 2006, **25**, 1399–1411; (*d*) G. D. Jones, C. McFarland, T. J. Anderson and D. A. Vicic, *Chem. Commun.*, 2005, 4211–4213.

9 G. Y. Yin, I. Kalvet, U. Englert and F. Schoenebeck, *J. Am. Chem. Soc.*, 2015, **137**, 4164–4172.

10 (*a*) V. B. Phapale and D. J. Cárdenas, *Chem. Soc. Rev.*, 2009, **38**, 1598–1607; (*b*) C.-Y. Lin and P. P. Power, *Chem. Soc. Rev.*, 2017, **46**, 5347–5399; (*c*) F.-S. Han, *Chem. Soc. Rev.*, 2013, **42**, 5270–5298; (*d*) V. P. Ananikov, *ACS Catal.*, 2015, **5**, 1964–1971; (*e*) N. Hazari, P. R. Melvin and M. M. Beromi, *Nat. Rev. Chem.*, 2017, **1**, 0025.

11 M. I. Lipschutz, X. Z. Yang, R. Chatterjee and T. D. Tilley, *J. Am. Chem. Soc.*, 2013, **135**, 15298–15301.

12 S. Miyazaki, Y. Koga, T. Matsumoto and K. Matsubara, *Chem. Commun.*, 2010, **46**, 1932–1934.

13 K. N. Zhing, M. Conda-Sheridan, S. R. Cooke and J. Louie, *Organometallics*, 2011, **30**, 2546–2552.

14 S. Nagao, T. Matsumoto, Y. Koga and K. Matsubara, *Chem. Lett.*, 2011, **40**, 1036–1038.

15 A. L. Zhang, S. Raje, J. G. Liu, X. Y. Li, R. Angamuthu, C.-H. Tung and W. G. Wang, *Organometallics*, 2017, **36**, 3135–3141.

16 J. S. Kim, J. H. Reibenspies and M. Y. Darensbourg, *J. Am. Chem. Soc.*, 1996, **118**, 4115–4123.

17 (*a*) T. L. James, D. M. Smith and R. H. Holm, *Inorg. Chem.*, 1994, **33**, 4869–4877; (*b*) Y.-M. Hsiao, S. S. Chojnacki, P. Hinton, J. H. Reibenspies and M. Y. Darensbourg, *Organometallics*, 1993, **12**, 870–875.

18 (*a*) C. Yoo and Y. Lee, *Angew. Chem., Int. Ed.*, 2017, **56**, 9502–9506; (*b*) P. L. Holland, T. R. Cundari, L. L. Perez, N. A. Eckert and R. J. Lachicotte, *J. Am. Chem. Soc.*, 2002, **124**, 14416–14424.

19 A. Bakac and J. H. Espenson, *J. Am. Chem. Soc.*, 1986, **108**, 713–719.

20 P. Stoppioni, A. Biliotti and R. Morassi, *J. Organomet. Chem.*, 1982, **236**, 119–122.

21 G. R. Fulmer, A. J. M. Miller, N. H. Sherden, H. E. Gottlieb, A. Nudelman, B. M. Stoltz, J. E. Bercaw and K. I. Goldberg, *Organometallics*, 2010, **29**, 2176–2179.

22 R. Kehoe, M. Mahadevan, A. Manzoor, G. McMurray, P. Wienefeld and M. C. Baird, *Organometallics*, 2018, **37**, 2450–2467.

23 O. Vechorkin, V. Proust and X. L. Hu, *J. Am. Chem. Soc.*, 2009, **131**, 9756–9766.

24 L. C. Silva, P. T. Gomes, L. F. Veiros, S. I. Pascu, M. T. Duarte, S. Namorado, J. R. Ascenso and A. R. Dias, *Organometallics*, 2006, **25**, 4391–4403.

25 R. Benn and G. Schroth, *Org. Magn. Reson.*, 1980, **14**, 435–438.

26 (*a*) N. M. Brunkan, D. M. Brestensky and W. D. Jones, *J. Am. Chem. Soc.*, 2004, **126**, 3627–3641; (*b*) B. Crociani, S. Antonaroli, P. Paoli and P. Rossi, *Dalton Trans.*, 2012, **41**, 12490–12500; (*c*) N. M. Brunkan and W. D. Jones, *J. Organomet. Chem.*, 2003, **683**, 77–82.
27 J. F. Hartwig, *Organotransition Metal Chemistry, from Bonding to Catalysis*, University Science Books, New York, 2010.
28 V. K. Ratheesh Kumar and K. R. Gopidas, *Tetrahedron Lett.*, 2011, **52**, 3102–3105.